The Structure of Quantization Noise from Sigma–Delta Modulation

JAMES C. CANDY, FELLOW, IEEE, AND OCONNELL J. BENJAMIN

Abstract—**When the sampling rate of a sigma–delta modulator far exceeds the frequencies of the input signal, its modulation noise is highly correlated with the amplitude of the input. We derive simple algebraic expressions for this noise and its spectrum in terms of the input amplitude. The results agree with measurements taken on a breadboard circuit.**

This work can be useful for designing oversampled analog to digital converters that use sigma–delta modulation for the primary conversion.

I. INTRODUCTION

QUANTIZATION noise introduced by delta modulation is easily analyzed when one assumes that overloading is avoided and that the noise is random [1]. The results of such analysis agree with practice provided the modulator has an active input, but the results are misleading for quiet inputs. It is the assumption of randomness that is faulty. When the input is steady the noise is highly colored, its spectrum appears as sets of distinct lines and the signal distortion is critically dependent on circuit conditions that determine whether or not strong lines lie in baseband.

The authoritative work on the structure of noise from delta modulation is that of Iwersen [2]. He gives a description of the noise spectrum and shows how it depends on imbalance between positive and negative step size and on the input signal.

Iwersen's work has been particularly useful for designing oversampled PCM encoders which make use of high speed delta modulation as the initial encoding [3]. The output of the modulator, when digitally filtered, is resampled at twice baseband frequency to provide the PCM. Deliberate imbalance of step size can greatly improve the idle channel resolution of these codecs [4].

The present work derives results for sigma-delta modulation that are closely related to those of Iwersen. The approach used in this analysis is different from Iwersen's and in some respects is more direct. We show that reasonable approximations provide very simple descriptions of the resolution of modulators that are sampled at a high frequency, and the results agree with practice. Before presenting this analysis, we describe measurements of noise from a real circuit. The main emphasis of this paper is on sigma-delta modulation because it is fast becoming the preferred modulation for oversampled codecs [4]-[8]. The Appendix shows how the analysis applies to ordinary delta modulation. The analysis and some of the results presented here also apply to the waiting-time problem described in [9].

Paper approved by the Editor for Data Communication Systems of the IEEE Communications Society for publication without oral presentation. Manuscript received January 21, 1981; revised April 29, 1981.

The authors are with Bell Laboratories, Holmdel, NJ 07733.

II. NOISE FROM SIGMA-DELTA MODULATION

Fig. 1 shows the circuit of a simple sigma-delta modulator, that accepts positive analog amplitudes and produces sequences of positive impulses. An impulse is generated, in time with the clock, whenever the integrated difference between the input and the output is positive. By this action the circuit regulates the rate at which impulses occur attempting to keep the average output equal to the average input. Zero input corresponds to no output impulses while maximum input corresponds to impulses generated at the clock rate. Then applied signals increase or decrease the rate its dynamic range where output impulses occur at one half the clock rate. Then applied signals increases or decreases the rate depending on whether they are positive or negative.

The output of the modulator is a digital representation of the signal, which can be demodulated by smoothing the impulses in a low-pass filter and removing the bias. In practical implementations the output pulses have finite duration but their shape can be allowed for in the design of the low-pass filter. Practical measurements described in this work came from a circuit that generates pulses lasting for a whole clock period, and they are smoothed in a low-pass filter that cuts off near 3.5 kHz.

When its input is steady, the modulator generates pulses in recurrent patterns that depend on the input level, and we expect the output to be noisy when repetition rates lie in baseband. Measured values of rms noise in baseband are plotted in Fig. 2 against input level, for three sampling rates. These graphs show that noise is largest when the modulator is biased near the ends of its range and next largest near the center. Indeed, most of the circuit's noise occurs in peaks adjacent to bias values that divide the dynamic range in small whole number ratios. Peaks of noise occur in pairs and are most prominent when the sampling rate is large compared to baseband. Arrows on the vertical axis of these graphs show average noise levels calculated from (35) of the Appendix.

For applications in communications it is advantageous to have low noise in the quiescent state; therefore, modulators should be biased to a quiet state away from the large peaks of noise. The advantage in doing so is demonstrated in Fig. 3 which shows the signal-to-noise ratio measured when the circuit was activated with a sinusoidal input for two conditions. One biased to the noisy state at the center of the dynamic range and the other to a relatively quiet state 1/20 of the range

0090-6778/81/0900-1316$00.75

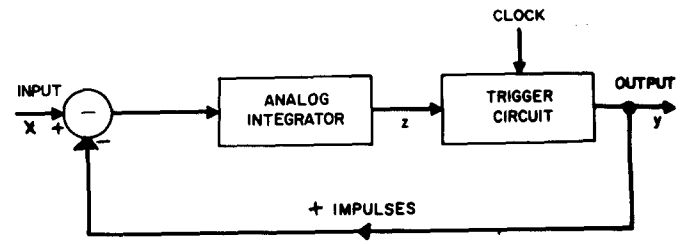

Fig. 1. An outline of a sigma-delta modulator, the trigger generates an impulse timed to the clock whenever z is positive.

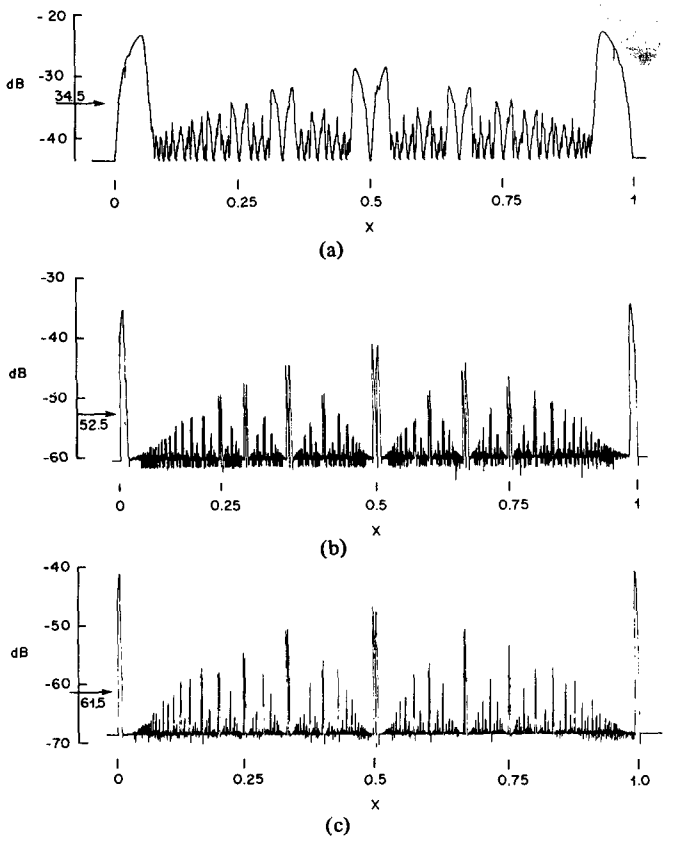

Fig. 2. Graphs of measured noise plotted against the level of dc input X. The active range is $0 < X < 1$ and for normal ac operation the modulator would be biased to $X = 0.5$. The arrow shows the expected average value of noise. Sampling rates are: (a) 64 kHz; (b) 256 kHz; (c) 512 kHz. Baseband is 3.5 kHz.

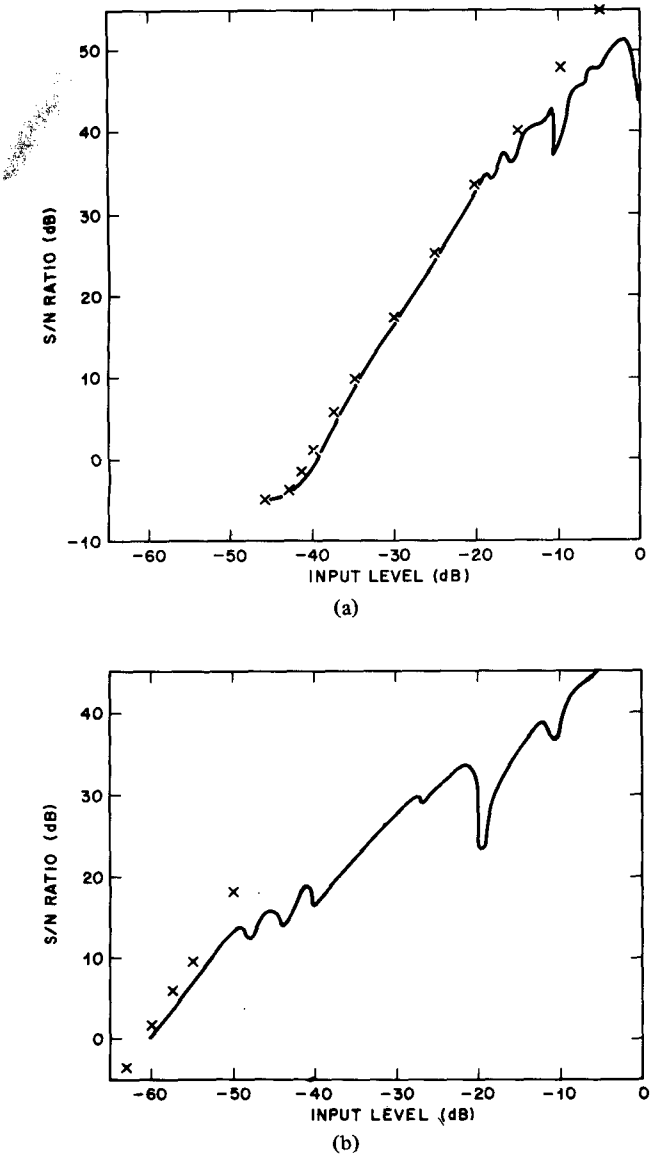

Fig. 3. Signal-to-noise ratio of a modulator with a 1.02 kHz sine wave input sampled at 256 kHz. X marks the expected values of idle channel S/N: (a) The modulator biased at center of its range. (b) The modulator biased at 11/20 of its range.

from center. The abscissa of these graphs is the amplitude of the input sine wave. Local depressions in the signal-to-noise ratio correspond to states where an extremity of the sine wave lies on a noise peak. For example, in Fig. 3(b), inputs that are a little larger than −20 dB touch the central noise peak.

The analysis we are about to present will enable these noise levels to be calculated, and because the structure of the noise is most noticeable at high sample rates, we will be concerned with sampling rates that far exceed baseband frequencies.

III. A MODEL FOR SIGMA-DELTA MODULATION

We now develop a model that is a convenient basis for analyzing the noise generated by sigma-delta modulation. First, consider the asynchronous modulator that uses no timing clocks, as shown in Fig. 4. We let x represent the input level and z represent the integrated difference between the input and the output, y. An impulse of magnitude A is generated at the output whenever z becomes positive. Fig. 5 shows representative waveforms of signals in this modulator. When x is constant, the error z is a regular sawtooth waveform and y a regular stream of impulses, both of frequency x/A.

Now modify the modulator to synchronize its output to a clock of period τ as in Fig. 1, where output impulses can occur only when the clock is present and z is positive. Waveforms in Fig. 6 show that the output impulses still occur at an average rate of x/A, (if $0 < x < A/\tau$), but each impulse is delayed from the corresponding asynchronous pulse in order to be aligned with the next clock. The synchronous sawtooth waveform z overshoots positively but returns to its asynchronous value after the impulse occurs.

An impulse waveform identical to y in Fig. 6 could be

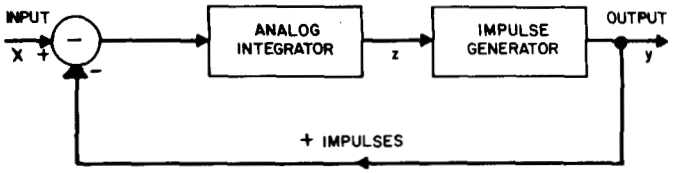

Fig. 4. The asynchronous modulator, an impulse is generated whenever z is positive.

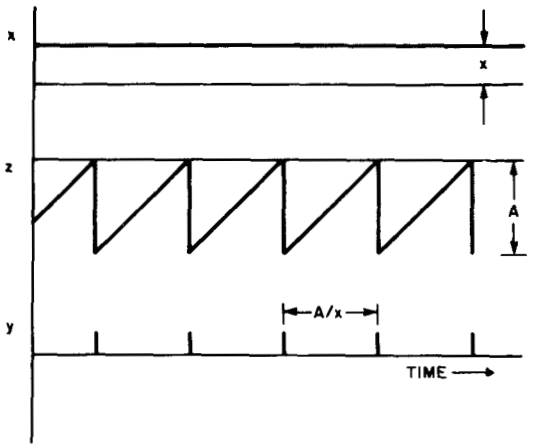

Fig. 5. Waveforms in the asynchronous modulator with dc input X.

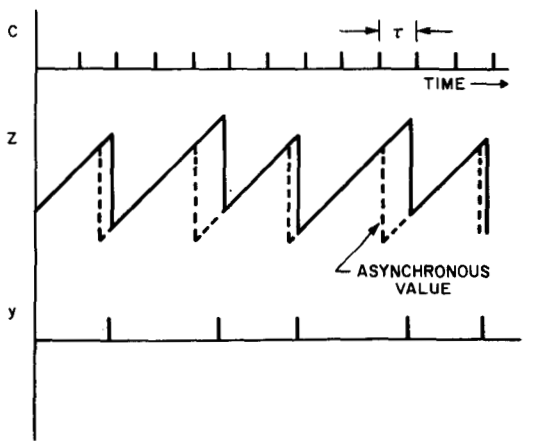

Fig. 6. Waveforms in the clocked modulator, with dc input X.

generated directly by sampling a regular sequence of rectangular pulses of frequency x/A and duration τ as shown in Fig. 7. This model would be inconvenient to implement, but it is very easy to describe mathematically; this we now do.

IV. ANALYSIS OF THE SIMPLIFIED MODEL

The range of inputs that the synchronous modulator can accommodate without saturating is $0 < x < A/\tau$. In order to have unit dynamic range we scale amplitudes to make $A/\tau = 1$, then, the input would normally be biased to the state where $x = \frac{1}{2}$.

The train of impulses that is the clock signal is represented by the expression

$$C(t) = \tau \sum_i \delta(t - i\tau) = \sum_k \exp\left(\frac{2\pi jkt}{\tau}\right). \tag{1}$$

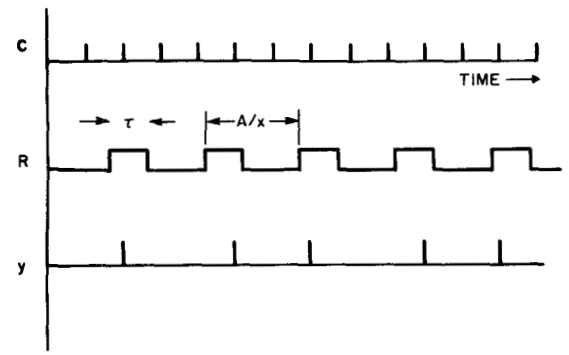

Fig. 7. A sampling system that produces the same output as does the clocked modulator.

Similarly, the rectangular wave in Fig. 7 can be expressed as

$$R(t) = \sum_i \int dt \left\{ \delta\left(t - t_0 - \frac{i\tau}{x}\right) - \delta\left(t - t_0 - \tau - \frac{i\tau}{x}\right) \right\} \tag{2}$$

where the delay t_0 is determined by initial conditions of the modulator. The Fourier series representation of the rectangular wave can now be written in the forms

$$R(t) = \frac{x}{\tau} \sum_l \int dt \left\{ \exp\left(2\pi j \frac{lx}{\tau}(t - t_0)\right) - \exp\left(2\pi j \frac{lx}{\tau}(t - t_0 - \tau)\right) \right\} \tag{3}$$

$$= \sum_l \frac{\sin(\pi lx)}{\pi l} \exp\left(2\pi jl \frac{x}{\tau}\left(t - t_0 - \frac{\tau}{2}\right)\right). \tag{4}$$

The output, R sampled by C, is given by the product of $C(t)$ and $R(t)$.

$$y(t) = \sum_l \sum_k \frac{\sin(\pi lx)}{\pi l} \exp\left(2\pi j \frac{(lx + k)}{\tau} t\right). \tag{5}$$

In this last equation the constant delay $(t_0 + (\tau/2))$ has been ignored.

The result (5) represents the output signal as sets of spectral lines of frequency

$$f = \left(\frac{lx + k}{\tau}\right). \tag{6}$$

Appendix II shows that this agrees with Iwersen's result for delta modulation [2]. Now recall that all the useful information in a sampled wave is contained in a band of frequency equal to half the sample rate

$$f \leq \frac{1}{2\tau}. \tag{7}$$

In order to study this band we direct our attention to those values of l and k that satisfy

$$|lx + k| \leqslant \tfrac{1}{2} \tag{8}$$

and thereby eliminate the parameter k.

At this point it is useful to introduce the following notation: $I(v)$ will represent the nearest integer to the real number v and $[v]$ will represent the fractional roundoff, that is,

$$[v] = (v - I(v)) \tag{9}$$

where

$$-0.5 < (v - I(v)) \leqslant 0.5.$$

For a component of (5) to lie in the band (7) requires that

$$k = -I(lx), \tag{10}$$

and its frequency can be expressed as

$$f_1 = \frac{[lx]}{\tau}. \tag{11}$$

Thus, the components of y that lie in the half sample band of frequencies can be expressed as

$$y_1(x) = x + 2\sum_{l=1}^{\infty} \frac{\sin(\pi lx)}{\pi l} \cos\left(2\pi[lx]\frac{t}{\tau}\right). \tag{12}$$

The first term in this expression represents the useful output; the second term is modulation noise.

V. BASEBAND NOISE

For the noise component of y at frequency f to lie in baseband f_0, $0 \leqslant f < f_0 \leqslant \frac{1}{2}\tau$, requires that

$$f\tau = |[lx]| < f_0\tau. \tag{13}$$

The power associated with that component is given by the expression

$$P_1(lx) = 2\frac{\sin^2(\pi[lx])}{(\pi l)^2} \tag{14}$$

which agrees with the result (3a) in [4]. This noise power will tend to be largest when l is small, therefore, in order to examine the major properties of the noise, we want to locate those values of x in the range $0 \leqslant x < 1$ that satisfy (13) with small values of l.

We shall assume that the net power is given by the sum of powers in individual components because situations where components have precisely the same frequency are very unusual.

Notice in Fig. 2 that the baseband noise occurs predominantly in narrow peaks adjacent to integer divisions of the signal range, particularly when τf_0 is small. Let us now study the noise in the vicinity of the m/n division by letting

$$x = \left(\frac{m}{n} + v\right) \tag{15}$$

where $m \leqslant n$ are incommensurate integers and v a deviation. In order for x to locate major peaks of noise, sensible ranges for these parameters are relatively coarse divisions compared to the oversampling ratio

$$\frac{1}{n} > f_0\tau \tag{16}$$

and v small. Its true range will emerge as result (19).

Substituting (15) in (13) requires that

$$[lx] = \left[l\left(\frac{m}{n} + v\right)\right] < f_0\tau. \tag{17}$$

When v is very small this condition can hold only when $m = 0$ or l is a whole number multiple of n, otherwise

$$\left[\frac{lm}{n}\right] \geqslant \frac{1}{n} > f_0\tau.$$

We now put

$$l = in \tag{18}$$

where i is a positive integer then

$$[lx] = [lv].$$

Then frequency components lie in baseband if

$$\tau f = [lx] = [lv] < f_0\tau. \tag{19}$$

We are particularly interested in the case where l is small, that is,

$$l = in < \frac{f_0\tau}{|v|}; \tag{20}$$

then

$$[lv] = lv. \tag{21}$$

The range of v that permits this condition to hold is

$$|v| < v_{\max} = \frac{f_0\tau}{n}. \tag{22}$$

There are many values of l that satisfy (19) without satisfying (20) but they are large. (For example, values near to $l = j/|v|$ where $j \geqslant 1$.) The noise power neglected by accepting condition (20) is of the order of one part in $(f_0\tau)^{-2}$. This is

small because in most applications of sigma-delta modulation $f_0\tau < 0.1$.

In order to obtain a simple expression for the noise power let us now consider modulators where $f_0\tau$ is small enough that

$$\sin(\pi f_0\tau) \approx \pi f_0\tau. \tag{23}$$

Then, using (21) and (14), the power in each baseband component that satisfies (20) may be written as

$$P_1(v) = 2v^2. \tag{24}$$

To get an expression for the total noise power at a given value of x we need to know the number of components that satisfy (21). This inequality may be written as

$$i < \frac{f_0\tau}{n|v|} = \frac{v_{max}}{|v|} \tag{25}$$

which sets the limit on the number of significant noise components in baseband. In particular, for v in the range

$$\frac{v_{max}}{(i_1+1)} < |v| \leqslant \frac{v_{max}}{i_1}$$

there are i_1 components of noise and the net baseband power is given by

$$P(v) = (2i_1v^2).$$

Fig. 8(a) shows a graph of calculated values of the net rms baseband noise $v\sqrt{2i}$, plotted against v. Fig. 8(b) shows the rms noise measured on a real circuit. The sharp corners in Fig. 8(a) are rounded in (b) because the practical filter used to define baseband does not have the abrupt cutoff that the theory assumes. The characteristic of the filter that was used is shown in Fig. 9. A useful approximation of the measured graph in Fig. 8(b) is obtained by assuming that i is not only an integer but also a real number equal to $v_{max}/|v|$; then

$$P(v) = 2|v|v_{max} = \frac{2f_0\tau}{n}|v|. \tag{26}$$

A pair of maxima occur in the noise when $|v| = v_{max}$, their amplitude is given by

$$P_{max}(n) = 2v_{max}{}^2 = 2\left(\frac{f_0\tau}{n}\right)^2. \tag{27}$$

Fig. 10 shows a graph plotted against $1/n$ of the rms noise maxima, taken from Fig. 2. The value of f_0 calculated from the slopes of this graph is 3.0 kHz which is reasonably well in accord with the corner frequency of the filter characteristic in Fig. 9.

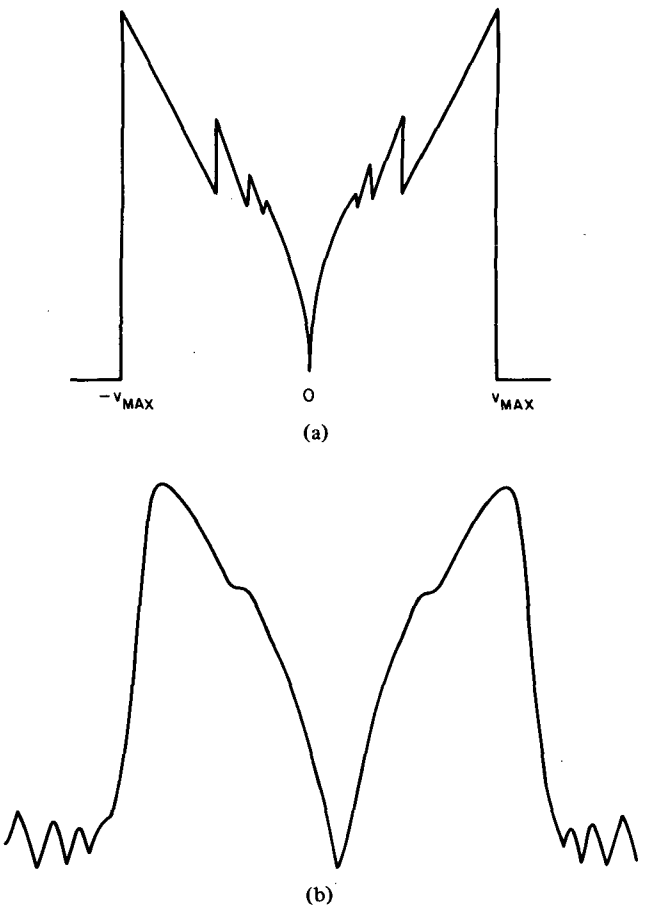

Fig. 8. An expanded view of a pair of peaks of noise. (a) Expected shape with ideal low-pass filter. (b) Measured shape with real baseband filter.

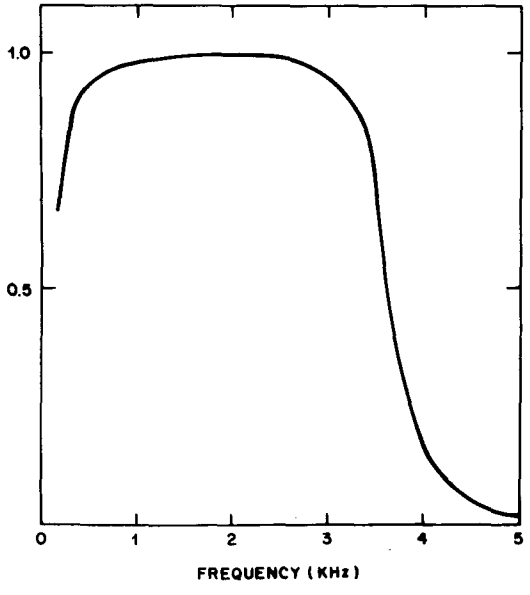

Fig. 9. Response of the low-pass filter that defines baseband in the experimental circuit. The analysis assumes an abruptly cutoff filter.

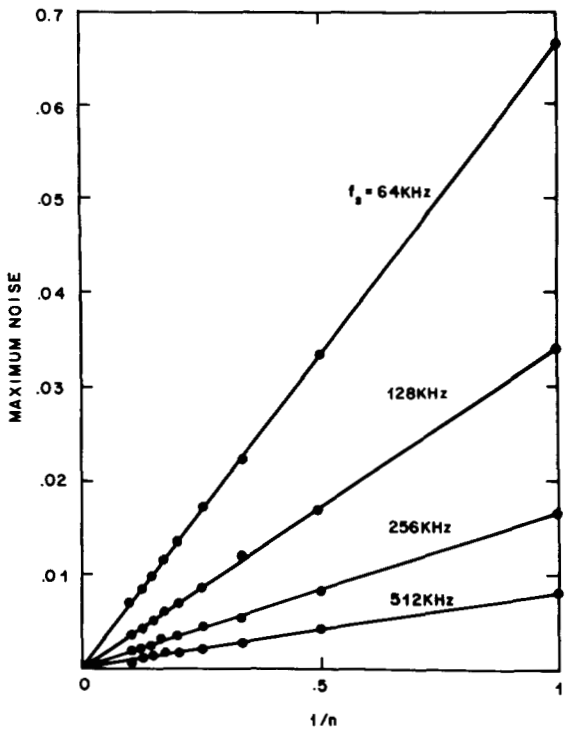

Fig. 10. The maximum rms values of noise in Fig. 2 plotted against $1/n$ for various sampling rates.

The total power in one peak of noise can be expressed as

$$P_T(n) = \sum_{i=1}^{\infty} \int_0^{\frac{v_{max}}{i}} 2v^2\, dv \tag{28}$$

$$= \tfrac{2}{3} {v_{max}}^2 \left(\sum_i \frac{1}{i^3}\right)$$

$$= 0.8 {v_{max}}^3 = 0.8 \left(\frac{f_0\tau}{n}\right)^3.$$

Eighty-three percent of this noise is contributed by the primary component for which $i_1 = 1$ (i.e., $l = n$).

Results (25)-(28) are all independent of the parameter m defined by (15); this fact agrees with the measurements presented as Fig. 2. Properties of the first peak at $x = 0$, for which $m = 0$, can be obtained by studying the final peak at $x = 1$, for which $n = 1$ because

$$\left\{l\left(\frac{m}{n} + v\right)\right\} = [lv]$$

for all l when $m = 0$ or $n = 1$.

VI. APPLICATIONS OF THE RESULTS

The results derived in the previous sections apply to modulators that have steady dc input signals. They may be used, however, for dynamic inputs that change slowly compared with the sampling rate. This assertion was confirmed by replotting the graphs of Fig. 3 for signal frequencies in the range 100 Hz to 3 kHz and noting no appreciable change. We may therefore express the net noise power for any input that changes slowly by

$$N^2 = \int_0^1 P(x)p(x)\, dx. \tag{29}$$

$P(x)$ is the noise for an input level x as given by (26) and $p(x)$ is the fraction of time that the input has value x. For sinusoidal input having amplitude A and dc offset x_0

$$p(x) = \frac{1}{\pi\sqrt{A^2 - (x - x_0)^2}}, \qquad |x - x_0| \leqslant A \tag{30}$$

$$= 0, \qquad \text{otherwise.}$$

To calculate the noise contributed by the two peaks in the region of input level $x = m/n$ we use (26) to get

$${N_1}^2(n) = \int_{-v_{max}}^{v_{max}} \frac{2}{\pi} \frac{v_{max}\,|v|\,dv}{\sqrt{A^2 - (x - x_0)^2}}. \tag{31}$$

Now we consider three examples that relate to properties of the graphs in Fig. 3.

Example 1: We will calculate the noise contributed by the pair of large peaks at the center of the range where $x = 1/2$. The modulator is assumed to be biased to the center $x_0 =$ and the input is a sine wave of amplitude A. To describe the noise peaks we put $n = 2$, $v_{max} = (f_0\tau)/2$ and $x = (1/2 + v)$, then (31) becomes

$${N_1}^2(2) = 2 \int_0^{v_1} \frac{2}{\pi} \frac{v_{max} v\, dv}{\sqrt{A^2 - v^2}} \tag{32}$$

where the range $v_1 = v_{max}$ *if* $A \geqslant v_{max}$ and $v_1 = A$, otherwise. It follows that

$${N_1}^2(2) = \frac{4v_{max}}{\pi} (A - \sqrt{A^2 - {v_{max}}^2}), \quad A \geqslant v_{max} \tag{33}$$

$$= \frac{4v_{max}A}{\pi}, \qquad A < v_{max}.$$

Selected values of the rms signal-to-noise ratio derived from (33) are shown on the graph in Fig. 3. We see good agreement for input amplitude below −20 dB. At larger amplitudes, noise from other peaks contribute strongly to the net impairment. We draw attention to the fact that some of the error predicted by (33) manifests itself as a loss of gain rather than as added noise. This loss is sometimes a significant part of the distortion and it has been included in the measurements reported in Fig. 3.

An interesting property of result (33) is the fact that when $A = v_{max}$ the signal-to-noise ratio is $\sqrt{\pi}/8 = -4.06$ dB independent of the sampling rate.

Example 2: We now consider the case where the modulator is biased to center $x_0 = 1/2$ and the input sine wave is about -9 dB ($A \approx 1/6$) below saturation. In this condition the noise peaks at center have little effect on resolution (see Example 1). The dominant noise is that for which $n = 3$, it distorts both extremes of the sine wave where $x = \frac{1}{3}$ and $\frac{2}{3}$. The noise power from these peaks is largest when the maximum noise lies on the extreme of the sine wave. This noise can be expressed as

$$N_1^2(3) = 2 \int_{-v_{max}}^{v_{max}} \frac{2}{\pi} \frac{v_{max} v\, dv}{\sqrt{(\frac{1}{6} + v_{max})^2 - (\frac{1}{6} + v)^2}}. \quad (34)$$

For 256 kHz sampling and 3 kHz baseband

$$v_{max} = \tfrac{1}{3} \tfrac{3}{256} = \tfrac{1}{256}.$$

We neglect v_{max} in comparison with $\frac{1}{3}$ to get

$$N_1^2(3) = \sqrt{3} \frac{4}{\pi} v_{max} \cdot \left[\int_0^{v_{max}} \frac{v\, dv}{\sqrt{v_{max} - v}} + \int_0^{v_{max}} \frac{v\, dv}{\sqrt{v_{max} + v}} \right]$$

$$= \frac{8}{\sqrt{3}\pi} (4 - \sqrt{2}) v_{max}^2 \sqrt{v_{max}}$$

and the signal-to-noise ratio = 35.8 dB. This compares with the measured value, 37 dB.

Example 3: With the modulator biased 1/20 of the range from center, we calculate the idle channel noise introduced by the two small peaks for which $n = 10$, $x = (11/20) + v$), $x_0 = 11/20$, and $v_{max} = (f_0\tau/10)$. Following the same reasoning as that of Example 1 the noise is given by (33). The expected signal-to-noise ratio plotted in Fig. 3(b) agrees with the measured value for small inputs.

VII. MULTILEVEL QUANTIZATION

Some sigma-delta modulators use multilevel quantization rather than the two level that we have considered. The analysis presented applies to such multilevel quantization provided that the net gain in the feedback loop [8] is unity and that signal amplitudes are scaled to make the step size unity.

Measurements on a real circuit indicate that changes of loop gain near unity have a weak effect on the noise. Indeed, modulators with gains in the range 0.7 – 1.3 all have similar noise structures.

With multilevel quantization the amplitude of the signal can far exceed the step size and the probability that the input has a particular value $p(x)$ is correspondingly reduced. This fact tends to whiten the net noise in multilevel modulators.

CONCLUDING REMARKS

We have demonstrated that simple formulas give good predictions of the resolution that can be obtained from sigma-delta modulators. The method is particularly useful for determining the resolution at certain critical states where just a few noise peaks of Fig. 2 dominate. These states usually set the minimum resolution of the modulator and are thus of most interest in the design of a circuit.

Complete graphs of the resolution, such as those given in Fig. 3, would be tedious to calculate; they are better obtained by simulation.

APPENDIX

ANALYSIS BASED ON RANDOM NOISE

We assume that the input is sufficiently active to make the quantization noise so random that it may [8] be represented as additive white noise E with power spectral density τe_0^2. The modulator is represented by the circuit in Fig. 11 and its action described by

$$Y_n = X_n + (E_n - E_{n-1}).$$

Thus, the rms spectral density of the noise added to the signal can be represented as

$$N(\omega) = \sqrt{\tau} e_0 (1 - \exp(-j\omega\tau))$$

and its magnitude expressed as

$$|N(\omega)| = 2\sqrt{\tau} e_0 \sin\left(\frac{\omega\tau}{2}\right).$$

The net rms noise in baseband N_0 is given by

$$N_0^2 = 4 e_0^2 \tau \int_0^{f_0} \sin^2(\pi f \tau)\, df$$

$$= 2 f_0 \tau e_0^2 (1 - \operatorname{sinc}(2\pi f_0 \tau)).$$

For oversampled modulators $f_0\tau \ll 1$, N_0 may be approximated by

$$N_0 = \frac{2\pi}{\sqrt{3}} e_0 (f_0\tau)^{3/2}.$$

The quantization noise E has uniform amplitude distribution in the range ± 0.5. Therefore, $e_0 = \frac{1}{\sqrt{6}}$. Thus, the rms baseband noise from an active modulator is expected to be

$$N_0 = \frac{\sqrt{2}\pi (f_0\tau)^{3/2}}{3}. \quad (35)$$

This value is marked on the graphs in Fig. 3.

Comparing N_0^2 with the noise power in each separate peak as given by (28) we find that the sum of the noise in the peaks is very nearly equal to N_0^2. About $\frac{3}{4}$ of this total is contained in the two peaks at the ends of the range. The two peaks at the center have about 0.1 of the total.

NOISE FROM ORDINARY DELTA MODULATION

Fig. 12(a) is a diagram of a delta modulator and Fig. 12(b) is an equivalent circuit based on the sigma-delta modulator.

In order to obtain a constant input to the sigma-delta

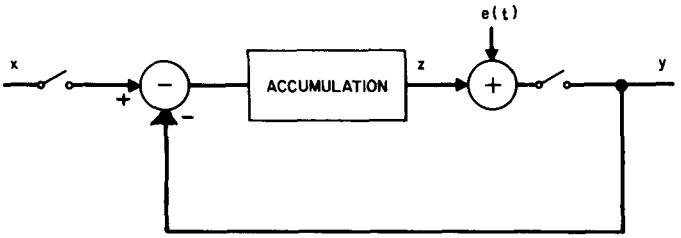

Fig. 11. A linear sampled data model of a sigma-delta modulator.

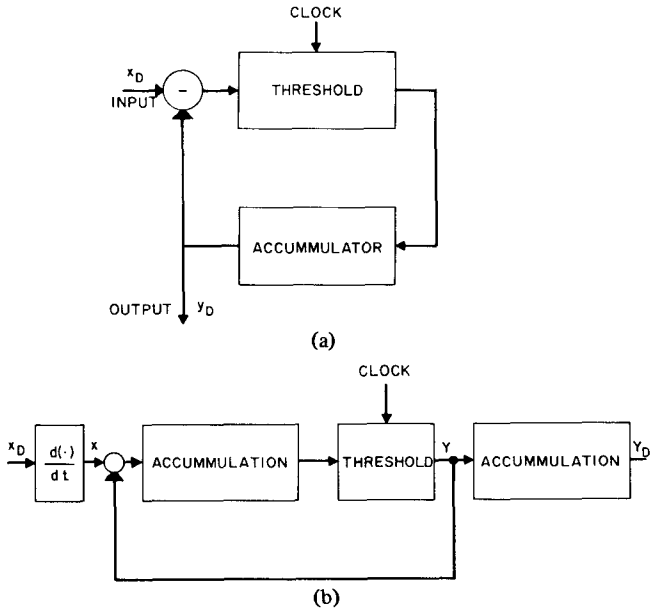

Fig. 12. (a) Schematic of a delta modulator. (b) An analog of a delta modulator that is based on sigma-delta modulation.

modulator a constant rate of change is required at the input to the delta modulator. Then the output of the sigma-delta modulator, given by (5), can be accumulated to give the delta modulator output. Such accumulation may be represented by

$$y_D(t) = \frac{y(t)}{1 - \exp(-2\pi j f \tau)}$$

$$= \sum_l \sum_k \frac{\sin(\pi l x) \exp\left(2\pi j (lx + \kappa) \frac{t}{\tau}\right)}{\pi l (1 - \exp(-2\pi j (lx + \kappa))}$$

$$y_D(t) = \sum_l \sum_\kappa \frac{\exp\left(2\pi j (lx + \kappa) \frac{t}{\tau}\right)}{2\pi j l (-1)^\kappa}.$$

Here, we have neglected the constant delays. This result agrees with Iwersen's when x represents rate of change of input signal.

ACKNOWLEDGMENT

The authors would like to thank W. H. Ninke and G. R. Ritchie for their helpful advice.

REFERENCES

[1] R. Steele, *Delta Modulation Systems*. New York: Wiley, 1975, ch. 3.

[2] J. E. Iwersen, "Calculated quantizing noise of single-integration delta modulation coders," *Bell Syst. Tech. J.*, vol. 48, pp. 2359–2389, Sept. 1969.

[3] D. J. Goodman and L. J. Greenstein, "Quantizing noise of DM/PCM encoders," *Bell Syst. Tech. J.*, vol. 52, pp. 183–204, Feb. 1973.

[4] T. Misawa, J. E. Iwersen, and J. G. Rush, "A single-chip CODEC with filters, architecture," in *Int. Conf. Commun. Rec.*, vol. 1, June 1980, pp. 30.5.1–30.5.6.

[5] J. C. Candy, Y. C. Ching, and D. S. Alexander, "Using triangularly weighted interpolation to get 13-bit PCM from a sigma-delta modulator," *IEEE Trans. Commun.*, vol. COM-24, pp. 1268–1275, Nov. 1976.

[6] J. D. Everhard, "A single-channel PCM codec," *IEEE J. Solid-State Circuits*, vol. SC-11, pp. 25–38, Feb. 1979.

[7] J. C. Candy, B. A. Wooley, and O. J. Benjamin, "A voiceband codec with digital filtering," *IEEE Trans. Commun.*, vol. COM-29, pp. 815–830, June 1981.

[8] R. C. Brainard and J. C. Candy, "Direct-feedback coders: Design and performance with television signals," *Proc. IEEE*, vol. 37, pp. 776–786, May 1969.

[9] *Transmission Systems for Communications*, 5th ed. Bell Telephone Laboratories, Inc., 1981.

★

James C. Candy (M'61–SM'74–F'76), for a photograph and biography, see page 830 of the June 1981 issue of this TRANSACTIONS.

★

Oconnell J. Benjamin, for a photograph and biography, see page 830 of the June 1981 issue of this TRANSACTIONS.